

## Iron Uptake and Iron-Repressible Polypeptides in *Yersinia pestis*

THOMAS S. LUCIER,<sup>1</sup>† JACQUELINE D. FETHERSTON,<sup>2</sup> ROBERT R. BRUBAKER,<sup>1</sup>  
AND ROBERT D. PERRY<sup>2\*</sup>

Department of Microbiology, Michigan State University, East Lansing, Michigan 48824-1101,<sup>1</sup> and Department of Microbiology and Immunology, University of Kentucky, Lexington, Kentucky 40536-0084<sup>2</sup>

Received 15 March 1996/Returned for modification 30 April 1996/Accepted 27 May 1996

**Pigmented (Pgm<sup>+</sup>) cells of *Yersinia pestis* are virulent, are sensitive to pesticin, adsorb exogenous hemin at 26°C (Hms<sup>+</sup>), produce iron-repressible outer membrane proteins, and grow at 37°C in iron-deficient media. These traits are lost upon spontaneous deletion of a chromosomal 102-kb *pgm* locus (Pgm<sup>-</sup>). Here we demonstrate that an Hms<sup>+</sup> but pesticin-resistant (Pst<sup>r</sup>) mutant acquired a 5-bp deletion in the pesticin receptor gene (*psn*) encoding IrpB to IrpD. Growth and assimilation of iron by Pgm<sup>-</sup> and Hms<sup>+</sup> Pst<sup>r</sup> mutants were markedly inhibited by ferrous chelators at 37°C; inhibition by ferric and ferrous chelators was less effective at 26°C. Iron-deficient growth at 26°C induced iron-regulated outer membrane proteins of 34, 28.5, and 22.5 kDa and periplasmic polypeptides of 33.5 and 30 kDa. These findings provide a basis for understanding the *psn*-driven system of iron uptake, indicate the existence of at least one additional 26°C-dependent iron assimilation system, and define over 30 iron-repressible proteins in *Y. pestis*.**

Pathogenic bacteria encounter iron-deficient growth conditions in vivo because of host iron- and heme-binding compounds (e.g., transferrin, lactoferrin, ferritin, hemopexin, albumin, myoglobin, hemoglobin, and haptoglobin) that control the availability of this essential trace nutrient (13, 15, 27). To obtain the iron necessary for growth in mammalian environments, microorganisms have developed disparate and elaborate iron acquisition systems. Numerous siderophore-mediated iron transport systems for acquiring chelated inorganic iron have been described (13, 15, 27, 31). However, certain pathogens utilize siderophore-independent mechanisms to obtain iron from transferrin, lactoferrin, and ferritin (7, 13, 27). Also, other virulent species utilize a variety of heme compounds as nutritional sources of iron (13, 18, 24, 27, 31, 34). Iron transport systems typically require outer membrane (OM) receptors along with periplasmic and inner (cytoplasmic) membrane (IM) proteins to internalize iron. Production of these proteins is often regulated by iron availability such that iron transport genes are highly expressed only during iron deprivation (13, 29, 31). Many of these uptake systems are also utilized by bacteriocins (9, 29) or bacteriophages (29, 31) to gain access to the bacterial cell. In most enteric organisms, expression of these peptides and other components of transport systems is regulated by the ferric uptake regulation (Fur) protein, which acts as both the iron status sensor and a negative regulator of transcription (15, 31).

Cells of *Yersinia pestis* can utilize ferritin, hemin, and various heme-containing proteins as sole sources of iron (35, 41, 43). In vitro growth of *Y. pestis* in iron-deficient media results in Fur-regulated and/or other iron-regulated expression of numerous proteins (5, 41, 42). For example, Carniel et al. (5) first reported that pathogenic strains express a 70-kDa protein and two high-molecular-mass iron-regulated proteins termed HMWP1 and HMWP2 of 240 and 190 kDa, respectively. Sikkema and Brubaker (41) detected five major iron-regulated OM proteins (IrpA to IrpE, 80.1, 68.8, 67.4, 69.1, and 65.1 kDa, respec-

tively). Over 20 iron-repressible and 6 iron-inducible proteins have been detected in *Y. pestis* (42). Of these, IrpB to IrpE, HMWP1, and HMWP2 are specific to pigmented (Pgm<sup>+</sup>) cells of *Y. pestis* and appear to be required for the growth of these organisms in iron-chelated media at 37°C (6, 10, 11, 41).

The Pgm<sup>+</sup> phenotype of *Y. pestis* encompasses several traits, including adsorption of large quantities of hemin (Hms<sup>+</sup>) in the OM at 26°C (21, 36) mediated by expression of several unique polypeptides (32, 33, 41, 46), production of several iron-regulated proteins (10, 11, 41), ability to grow in iron-chelated media at 37°C (10, 40, 41), virulence in mice infected by peripheral routes of injection (22, 48), and sensitivity to the bacteriocin pesticin (Pst<sup>s</sup>) (3, 48). Spontaneous nonpigmented (Pgm<sup>-</sup>) mutants of *Y. pestis* arise as a consequence of a high-frequency (10<sup>-5</sup>) chromosomal deletion of ~102 kb (3, 12, 26) and fail to express any of these characteristics. A rare Hms<sup>+</sup> but pesticin-resistant (Pst<sup>r</sup>) mutant of *Y. pestis* (strain K115-B) that had not experienced this deletion (26) failed to express IrpB to IrpE and was unable to grow in an iron-chelated medium at 37°C (41). The original suggestion that one or more of these proteins may serve as the pesticin receptor and play a role in iron transport (41) has been demonstrated in *Y. pestis* (10) and *Y. enterocolitica* (38). The pesticin receptor gene (*psn* in *Y. pestis*) has been cloned, sequenced, and shown to encode IrpC, with IrpB and IrpD likely being modifications of IrpC. An in-frame *psn* deletion mutant lost the ability to grow at 37°C in an iron-deficient medium (10). Functional separation of this system from hemin storage is indicated by the existence of the Hms<sup>+</sup> Pst<sup>r</sup> mutant (41), by the ability of the cloned *hmsHFR* locus to restore hemin storage but not Pst<sup>s</sup> to a Pgm<sup>-</sup> mutant (37), and by the occurrence of strains of *Y. pseudotuberculosis* (48), *Y. enterocolitica* (48), and *Escherichia coli* (3) that are normally Hms<sup>-</sup> Pst<sup>s</sup>. Conjugal transfer of DNA which restores Pst<sup>s</sup> but not the Hms<sup>+</sup> trait also restores virulence in mice infected via peripheral routes of injection (23). Consequently, the iron uptake system associated with the Pst<sup>s</sup> and Pgm<sup>+</sup> phenotypes may be critical for virulence in a mammalian host.

In this study, we determined the genetic basis accounting for the Hms<sup>+</sup> Pst<sup>r</sup> mutant *Y. pestis* K115-B, identified and localized additional iron-repressible polypeptides, and examined the regulation of these proteins by temperature. We also ex-

\* Corresponding author. Phone: (606) 323-6341. Fax: (606) 257-8994. Electronic mail address: rdp@seqanal.mi.uky.edu.

† Present address: Department of Pediatrics, University of North Carolina, Chapel Hill, NC 27599.

TABLE 1. *Y. pestis* strains and recombinant plasmids used in this study

Bacterium or plasmid	Relevant characteristics <sup>a</sup>	Reference(s) or source
<i>Y. pestis</i> strains		
KIM6+	pMT1, pPCP1, Lcr <sup>-</sup> Pst <sup>I</sup> <i>pgm</i> <sup>+</sup>	11, 12, 26
KIM6-2046.1	pMT1, pPCP1, Lcr <sup>-</sup> Pst <sup>I</sup> Km <sup>r</sup> <i>hms</i> <sup>+</sup> <i>psn</i> <sup>+</sup> <i>irp2::kan</i> HMWP1 <sup>-</sup>	10
K115+	pMT1, Pst <sup>S</sup> Lcr <sup>-</sup> <i>pgm</i> <sup>+</sup> Leu and Pro auxotroph, derived from KIM6+	26, 41
K115-A	pMT1, Pst <sup>I</sup> Lcr <sup>-</sup> $\Delta$ <i>pgm</i> Leu and Pro auxotroph, derived from K115+	26, 41
K115-B	pMT1, Pst <sup>I</sup> Lcr <sup>-</sup> <i>hms</i> <sup>+</sup> <i>psn115B</i> Leu and Pro auxotroph, derived from K115+	26, 41, this study
K115-B(pPSN13.1)	pMT1, Cm <sup>r</sup> Pst <sup>S</sup> Lcr <sup>-</sup> <i>hms</i> <sup>+</sup> <i>psn115B</i> <i>psn</i> <sup>+</sup> Leu and Pro auxotroph, derived from K115-B	This study
Plasmids		
pACYC184	Cm <sup>r</sup> Tc <sup>r</sup> cloning vector	1
pUKAN19	Km <sup>r</sup> Ap <sup>r</sup> cloning vector, 1.68-kb <i>Bam</i> HI <i>kan</i> fragment from mini- <i>kan</i> (49) inserted into pUC19	This study
pPSN4	Ap <sup>r</sup> <i>psn</i> <sup>+</sup> , 4.4-kb <i>Bam</i> HI- <i>Pst</i> I fragment from pPSN2 inserted into pUC18	10
pPSN11	Ap <sup>r</sup> , 3.5-kb <i>Eco</i> RI fragment from pPSN2 inserted into pBGL2	This study
pPSN13.1	Cm <sup>r</sup> <i>psn</i> <sup>+</sup> , 4.2-kb <i>Hind</i> III- <i>Sal</i> I fragment from pPSN4 inserted into pACYC184	This study
pSDR498.4	Ap <sup>r</sup> <i>psn</i> <sup>+</sup> , 23-kb <i>Bgl</i> II fragment from pSDR498 inserted into pBGL2	10, 11
pDPSN1	Ap <sup>r</sup> <i>psn115B</i> , 4.2-kb <i>Pst</i> I- <i>Sal</i> I fragment from K115-B inserted into <i>Pst</i> I- <i>Xho</i> I site of pUKAN19	This study
pDPSN2	Ap <sup>r</sup> , <i>psn</i> <sup>+</sup> - <i>psn115B</i> hybrid, 1.8-kb <i>Eco</i> RI fragment from pPSN4 inserted into pDPSN1	This study
pDPSN2.1	Ap <sup>r</sup> <i>psn</i> <sup>+</sup> - <i>psn115B</i> hybrid, 0.4-kb <i>Kpn</i> I- <i>Sma</i> I fragment from pPSN4 inserted into pDPSN1	This study
pDPSN3	Ap <sup>r</sup> , <i>psn</i> <sup>+</sup> - <i>psn115B</i> hybrid, 1.1-kb <i>Kpn</i> I- <i>Bcl</i> II fragment from pPSN4 inserted into pDPSN1	This study
pDPSN4	Ap <sup>r</sup> , <i>psn</i> <sup>+</sup> - <i>psn115B</i> hybrid, 1.5-kb <i>Kpn</i> I- <i>Bcl</i> II fragment from pDPSN1 inserted into pPSN4	This study

<sup>a</sup> Endogenous *Y. pestis* KIM strain plasmids include pMT1 (110 kb) and pPCP1 (9.5 kb). Pst<sup>I</sup>, Pst<sup>I</sup>, and Pst<sup>S</sup> indicate immunity (due to pesticin immunity protein encoded on pPCP1), resistance, and sensitivity to pesticin, respectively. The low-calcium response phenotype of *Yersinia* strains is indicated by Lcr<sup>+</sup> or Lcr<sup>-</sup>. Ap<sup>r</sup>, Cm<sup>r</sup>, Km<sup>r</sup>, and Tc<sup>r</sup> indicate resistance to ampicillin, chloramphenicol, kanamycin, and tetracycline, respectively.

explored the ability of *Y. pestis* cells to obtain iron from selected iron chelators and the efficiency of an independent 26°C iron uptake system.

#### MATERIALS AND METHODS

**Bacteria and plasmids.** Characteristics of the *Y. pestis* strains, as well as the recombinant plasmids, used in this study are detailed in Table 1. A plus sign behind a *Y. pestis* strain designation indicates a completely intact *Pgm*<sup>+</sup> phenotype which includes the hemin storage (*hms*) locus, *irp2* (encoding HMWP2), and *psn* genes. *Pgm*<sup>-</sup> or  $\Delta$ *pgm* refers to *Y. pestis* strains that have undergone the ~102-kb chromosomal deletion of the *pgm* locus (11, 12, 26). The *Hms*<sup>+</sup> phenotype of *Y. pestis* strains was confirmed on Congo red agar (47). *E. coli* DH5 $\alpha$ , GM272, and XL-1 Blue were used as hosts for plasmids or bacteriophage (1, 39).

**Cultivation of *Y. pestis* and *E. coli* cells.** Growth of bacterial strains stored at -20°C in buffered glycerol was initiated on Tryptose blood agar base (Difco Laboratories) or Congo red agar for *Y. pestis* and on Luria broth solidified with agar for *E. coli*. For DNA isolation or pesticin sensitivity testing, *Yersinia* strains were grown in liquid heart infusion broth (Difco Laboratories) and *E. coli* strains were grown in Luria broth. All bacteria harboring antibiotic resistances were cultivated with the appropriate antibiotic (concentrations: 50  $\mu$ g/ml for ampicillin, kanamycin, and chloramphenicol and 12.5  $\mu$ g/ml for tetracycline).

For growth response studies under various iron conditions, all glassware was acid cleaned in saturated chromic acid and copiously rinsed with distilled, deionized H<sub>2</sub>O. All reagents were prepared in distilled, deionized H<sub>2</sub>O (Milli-Q [Millipore Corp.] or Nanopure [Barnstead]). *Yersinia* strains were cultivated in one of three chemically defined media. Modified Higuchi medium (50) and modified MOPS (3-*N*-morpholinopropanesulfonic acid) medium (35) were made iron deficient by omitting FeSO<sub>4</sub> during their preparation and by extraction with 8-hydroxyquinoline prior to addition of magnesium salts (35). The resulting media contained 0.3 to 1.0  $\mu$ M iron as determined on a SpectrAA Zeeman atomic absorption spectrophotometer (Varian Techtron Pty.). PMH medium was deferrated by the batch Chexel-100 (Bio-Rad) method, which results in a residual iron content of ~0.3  $\mu$ M (43). All of these chemically defined media are iron deficient unless iron supplementation is specified. Media were made iron replete by subsequent addition of FeCl<sub>3</sub> to 20  $\mu$ M (PMH medium) or FeCl<sub>2</sub> to 50  $\mu$ M (modified Higuchi medium and modified MOPS medium).

Following retrieval of bacteria from stock cultures, *Y. pestis* cells were grown overnight in iron-replete liquid modified Higuchi or MOPS medium at 26°C and aerated at 200 rpm in a G76 gyratory water bath shaker (New Brunswick Scientific Co.). Bacteria were harvested by centrifugation, washed twice with iron-deficient medium, and used to inoculate fresh iron-replete or iron-deficient medium to an optical density at 620 nm (OD<sub>620</sub>) of 0.1 (~10<sup>8</sup> cells per ml) by using a Gilford spectrophotometer. These cultures were grown at 26 or 37°C to an OD<sub>620</sub> of 1.0 and used to inoculate fresh cultures to the same concentration. Cells from the final culture were harvested for use in various tests during the late log phase. For electrophoretic analysis of radiolabelled proteins, cells were

grown in modified Higuchi medium supplemented with 20  $\mu$ Ci of L-[<sup>35</sup>S]methionine per ml as previously described (41).

To assay the ability to grow at 37°C under iron-deficient conditions, cells were cultivated at 37°C in deferrated liquid PMH medium for six to eight generations and then streaked onto solidified PMH medium supplemented with 0.5 mM NaCO<sub>3</sub>, 0.01 mM MnCl<sub>2</sub>, and 4 mM CaCl<sub>2</sub> (PMH-S). PMH-S inhibits growth of cells defective in iron accumulation, presumably by CaCl<sub>2</sub> precipitation of iron (10). To test for growth-stimulatory activity of culture supernatants, ~10<sup>7</sup> iron-deficient cells of *Y. pestis* KIM6-2046.1 (*irp2::kan*) were seeded onto PMH-S plates, 1-mm-diameter wells were filled (~20  $\mu$ l) with filtered supernatants from iron-deficient cultures, and the plates were incubated at 37°C (10).

**Gradient plates.** Gradient plates were prepared with modified MOPS solidified with 1% Noble agar (Difco). This medium lacks molecules which could compete effectively for residual iron with the chelators being tested (35). Stock solutions of the various iron chelators, in a 100-fold excess of the concentration needed in plates, were prepared in distilled, deionized H<sub>2</sub>O and filter sterilized. Stock solutions of sodium citrate and sodium PP<sub>i</sub> were extracted with 8-hydroxyquinoline to remove contaminating iron. Solutions of nitrotriacetic acid, 2,2'-dipyridyl, conalbumin, bathophenanthroline disulfonic acid, and desferrioxamine B (Desferal; Ciba Pharmaceutical Co.) were not deferrated prior to use. Twenty milliliters of medium containing a chelator was poured onto each 100-mm-wide plate and allowed to solidify while the plate was inclined, and then a 20-ml top layer (lacking any iron chelator) was poured onto the plate and allowed to solidify while the plate was on a level surface. This resulted in increasing concentrations of the chelator across the plate. Control plates had a basal layer which lacked iron chelators.

To inoculate the gradient plates, cells were grown to an OD<sub>620</sub> of 1.0 in modified MOPS medium as described above and diluted 1:100 in fresh modified MOPS medium, and 20  $\mu$ l of the suspension (~2  $\times$  10<sup>5</sup> CFU/ml) was streaked across the gradient. Plates were incubated at either 26 or 37°C, and the distance of cell growth along the gradient was recorded daily for 4 days, after which no further growth was observed. All strains grew on control plates lacking chelators, and growth across all chelator gradients was restored by inclusion of 50  $\mu$ M hemin or 100  $\mu$ M FeCl<sub>2</sub> in the overlayer, indicating that inhibition was caused by iron deprivation rather than toxicity of the chelators. Replicate plating with individual iron chelators was very reproducible (data not shown).

**Iron uptake assays.** *Y. pestis* K115+ (*Pgm*<sup>+</sup>), K115-A (*Pgm*<sup>-</sup>), or K115-B (*Hms*<sup>+</sup> *Pst*<sup>I</sup>) cells were grown in iron-deficient or iron-replete modified Higuchi medium to an OD<sub>620</sub> of 1.0 as described above. Subsequent uptake assays were adapted from previously described methods (8, 35). Briefly, cells were harvested by centrifugation, washed twice, and resuspended to an OD<sub>620</sub> of 7.0 in deferrated uptake buffer (25 mM *N*-2-hydroxyethylpiperazine-*N'*-2-ethanesulfonic acid [HEPES, pH 7.4], 2.5 mM K<sub>2</sub>HPO<sub>4</sub>, 20 mM MgCl<sub>2</sub>, 10 mM glucose extracted with 8-hydroxyquinoline). The iron content of the uptake buffer was 0.5 to 1.0  $\mu$ M as determined by atomic absorption spectrophotometry. Cells were kept on ice in this buffer for no longer than 40 min prior to initiation of the uptake assay.

To perform an assay, a 1.0-ml volume of cells was added to 8.9 ml of uptake buffer and acclimated for 10 min at either 26 or 37°C before 0.1 ml of uptake buffer containing 5.0  $\mu\text{Ci}$  of  $^{55}\text{FeCl}_3$  per ml (NEN Research Products) was added and timing was begun. The activity of the uptake buffer was 0.05  $\mu\text{Ci}/\text{ml}$  for a concentration of 30 pM  $^{55}\text{Fe}$ . Samples of 0.5 ml were withdrawn at regular intervals, filtered (0.22- $\mu\text{m}$  pore size), washed once with 5.0 ml of uptake buffer less glucose with 0.2 mM nitrilotriacetic acid to remove unabsorbed iron, and counted in a Packard Tri-Carb scintillation spectrometer. Protein concentrations in uptake assays were determined by the method of Lowry et al. (25).

**Protein analysis.** After growth in modified Higuchi medium, fractionation of all *Yersinia* strains was performed by a slightly modified form of the method of Straley and Brubaker (45). Briefly, cells were harvested by centrifugation and suspended in a 0.75 M sucrose buffer. Conversion to spheroplasts occurred during treatment with lysozyme and rapid dilution with low-molarity EDTA. Centrifugation separated spheroplasts from periplasm, and the later fractions were filtered and concentrated by precipitation in cold 10% trichloroacetic acid. Spheroplasts were disrupted by sonication, intact cells were removed by centrifugation, and the supernatant was separated into cytoplasmic and membrane fractions by centrifugation (240,000  $\times$  g, 3 h) in 0.25 M sucrose buffer. Cytoplasmic fractions did not require concentration prior to electrophoretic analysis. Pelleted membrane fractions were suspended and separated into IMs and OMs by isopycnic sucrose density gradient centrifugation. IMs and OMs were concentrated by centrifugation (190,000  $\times$  g, 4 h) in wash buffer (50 mM Tris-HCl [pH 6.8], 10 mM  $\text{MgCl}_2$ , 0.2 mM dithiothreitol). Previously, IM contamination of OM preparations was approximately 3% and the reverse ranged from 5 to 38% (45). As judged by sodium dodecyl sulfate (SDS)-polyacrylamide gel electrophoresis (PAGE) profiles, these levels of contamination appeared to be reduced when harvested cells were not washed with phosphate buffer. Lane SDS-PAGE and two-dimensional (2D) PAGE (isoelectric focusing followed by SDS-PAGE) were performed as previously described (30). Proteins were visualized by silver staining (28) or autoradiography followed by exposure to X-Omat AR film (Eastman Kodak Co.).

**In vitro DNA manipulations.** Plasmid DNA was introduced into *E. coli* by using a standard  $\text{CaCl}_2$  transformation protocol (1) and into *Yersinia* cells by electroporation as previously described (10). A rapid alkaline lysis plasmid isolation technique (2) was used to verify plasmid content. Large-scale isolation of highly purified plasmid DNA was obtained by differential DNA precipitation (19) of cleared cell lysates (2). Bacterial genomic DNA was isolated by a method utilizing lysozyme-SDS-proteinase K (1) and further purified by phenol and chloroform extractions. DNA restriction endonucleases, T4 DNA ligase, and calf intestinal alkaline phosphatase were used according to the manufacturers' specifications. Restriction enzyme-digested DNA fragments were separated by electrophoresis through 0.7% agarose and transferred, when required, to nitrocellulose by Southern blotting. Radiolabelled probes were generated by using a nick translation kit (Bethesda Research Laboratories). NEN Research Products was the source of [ $^{32}\text{P}$ ]dCTP. The probe DNA used for isolation of *psn115B* was a 2.4-kb *PstI-EcoRI* fragment from pPSN11. A 23-kb *BglIII* fragment from pSDR498.4, containing *psn*, part of *irp2*, and intervening DNA, was used as a probe to detect possible alterations in *ClaI*-digested genomic DNAs from *Pst*<sup>+</sup> and *Pst*<sup>-</sup> *Yersinia* strains. Southern blots and colony blots were probed under stringent hybridization conditions (1, 14, 42).

The 764-bp *BclI-EcoRV* fragment from the cloned *psn115B* gene was subcloned into M13mp18 and M13mp19 and transformed into XL-1 Blue cells. Bacteriophage were precipitated from culture supernatants with polyethylene glycol (39). Single-stranded phage DNA was sequenced by the dideoxynucleotide chain termination method (1, 39) using [ $^{35}\text{S}$ ]dATP (Amersham Corp.) and Sequenase Version 2.0 (U.S. Biochemical Corp.). Sequencing gels were prepared, electrophoresed, and visualized as previously described (10, 39).

**Pesticin sensitivity.** As previously described (44), a plate assay system was used to determine sensitivity or resistance to the yersinial bacteriocin pesticin.

**Nucleotide sequence accession numbers.** The GenBank accession number of the *psn115B* sequence determined in this study (see Fig. 2) is U27355.

## RESULTS

**Analysis of *Pst*<sup>+</sup> isolates.** In addition to the ~102-kb *Y. pestis* *pgm* locus deletion, alternative deletions involving the *Y. pestis* *irp2* gene have been observed (11, 12, 20). To detect any large DNA alterations, we performed Southern blot analysis with a DNA probe from the *psn-irp2* region. The hybridization pattern of strain K115-B (*Hms*<sup>+</sup> *Pst*<sup>+</sup>) was the same as that of its *Pst*<sup>+</sup> KIM115+ parent, while the hybridizing bands were absent from K115-A (*Pgm*<sup>-</sup>), since this region has been deleted (data not shown). Although the banding pattern of strain K115-B was unaltered in Southern blots, it produced HMWP1 and HMWP2 but not IrpB to IrpD, as shown by SDS-PAGE (Fig. 1).

We transformed strain K115-B with pPSN13.1, a plasmid

that contains the *Y. pestis* *psn* gene and converts *E. coli* DH5 $\alpha$  and *Y. pestis* KIM6 ( $\Delta$ *pgm*) to *Pst*<sup>+</sup> (data not shown). Five separate *Y. pestis* K115-B(pPSN13.1) transformants became *Pst*<sup>+</sup>. In addition, *Y. pestis* K115+ and K115-B(pPSN13.1) cells grew on PMH-S plates at 37°C while growth of K115-B cells was inhibited. PMH-S normally prevents growth at 37°C of *Y. pestis* cells possessing a  $\Delta$ *pgm*,  $\Delta$ *psn*, or *irp2::kan* mutation (10). Thus, the *Y. pestis* *psn* gene complemented the mutation to *Pst*<sup>+</sup> in *Y. pestis* K115-B. To determine if mutations had also occurred in the putative siderophore biosynthetic genes, growth-stimulating activity of culture supernatants for KIM6-2046.1 (*irp2::kan*) cells on PMH-S plates at 37°C was determined. Iron-deficient culture supernatants from K115+ and K115-B cells stimulated growth of KIM6-2046.1 cells, suggesting that synthesis of the putative siderophore of yersiniae was unaffected. In contrast, culture supernatant from K115-A cells had no stimulatory activity (data not shown). Collectively, these results indicate that the K115-B mutation lies within the *psn* gene.

**Cloning and characterization of the *Y. pestis* K115-B defective *psn* gene.** Genomic DNA from strain K115-B was isolated, digested with *Sall* and *PstI*, and ligated to the *PstI* and *XhoI* sites of pUKAN19. Clones containing the desired 4.2-kb *psn115B* fragment were identified by colony blotting (14) and confirmed for clone pDPSN1 by Southern blot hybridization and restriction enzyme analysis. In vitro transcription-translation analysis revealed that pDPSN1 expressed an ~40-kDa polypeptide consistent with a truncated product from *psn115B* (data not shown). This finding suggested that the mutation in K115-B is a small insertion, deletion, or base pair change that disrupts the normal reading frame. To localize the mutation site, we constructed recombinant plasmids containing hybrid *psn*<sup>+</sup>-*psn115B* genes (Table 1 and Fig. 2A), transformed them into *E. coli* DH5 $\alpha$ , and tested their pesticin sensitivity phenotype. This indicated that the *psn115B* mutation was within the 764-bp *BclI-EcoRI* fragment (Fig. 2A). DNA sequencing of the *BclI-EcoRV* fragment identified a 5-bp (GACCT) deletion that caused a reading frame shift promoting termination six amino acids after the deletion (Fig. 2B). The *psn115B* product should be 392 amino acids with an unprocessed molecular mass of ~43 kDa (40.6 kDa after removal of the signal peptide). This value agrees with the in vitro transcription-translation results.

**Iron uptake assays.** Expression of inducible iron uptake occurred in cells of *Y. pestis* K115+ (*Pgm*<sup>+</sup>), K115-A (*Pgm*<sup>-</sup>), and K115-B (*Hms*<sup>+</sup> *Pst*<sup>+</sup>) acclimated to growth in iron-deficient modified Higuchi medium at 37°C. However, initial rates of assimilation by *Pgm*<sup>+</sup> cells more than doubled those observed for both mutants (Fig. 3). Iron uptake by iron-starved K115+ cells began to show saturation by 45 min. Although the slower uptake by cells of both mutants continued through 90 min, they never assimilated the same levels of iron as parental cells (data not shown). In contrast, *Pgm*<sup>-</sup> cells acclimated to iron-deficient conditions at 26°C took in more iron than did *Pgm*<sup>+</sup> bacteria grown at 37°C (data not shown). As shown below, these differences were readily confirmed by diffusion in solid medium.

**Growth with iron chelators.** Gradient plates were developed to examine the ability of *Y. pestis* mutants K115-A (*Pgm*<sup>-</sup>) and K115-B (*Hms*<sup>+</sup> *Pst*<sup>+</sup>) to acquire iron from various chelators at 26 and 37°C. Under these conditions, cells on the surface were exposed to progressively higher concentrations of iron chelators along the length of the plate. As reported earlier by Sikkema and Brubaker (40, 41), K115+ cells showed greater growth at 37°C in the presence of citrate than did those of strain K115-A or K115-B. Similar results were obtained with

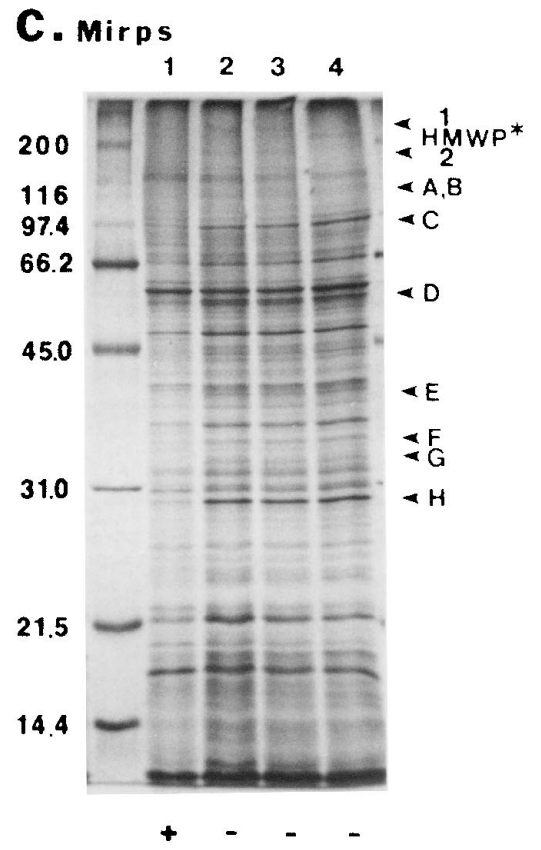
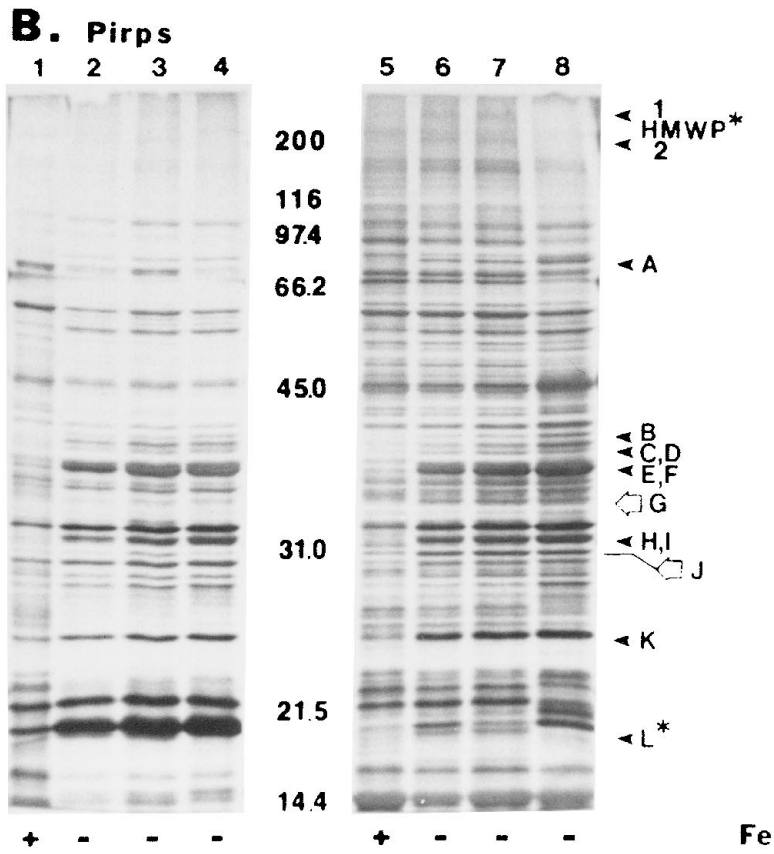
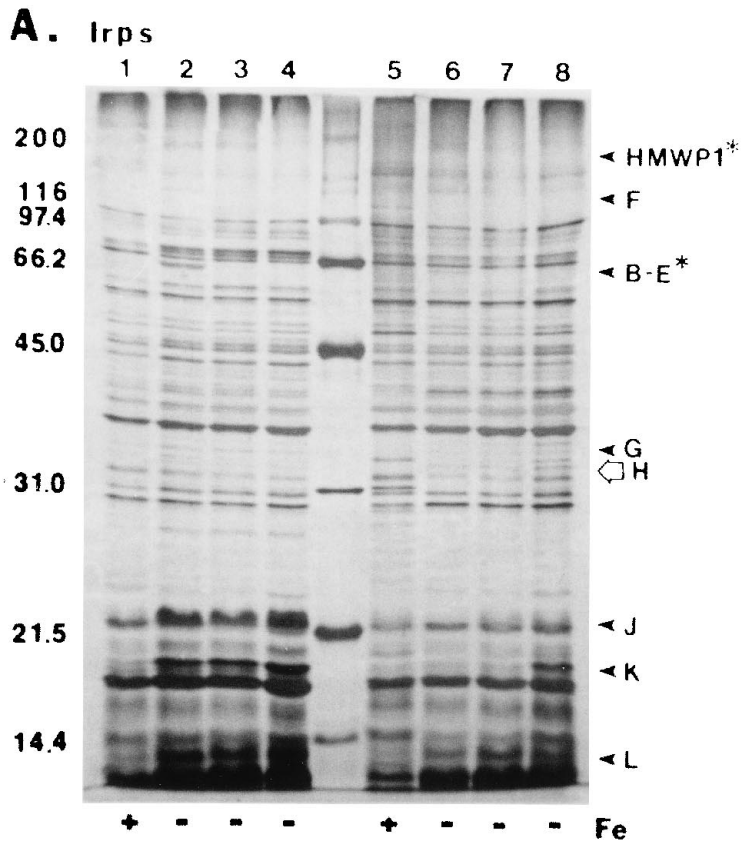


FIG. 1. SDS-PAGE profiles of OM (A), periplasmic (B), and IM (C) proteins from *Y. pestis* strains grown in modified Higuchi medium. Molecular masses are indicated in kilodaltons. Polypeptides were visualized by silver staining. Positions of detectable iron-repressible polypeptides in OMs (IrpS, gel A), periplasms (IrpP, gel B), and IMs (IrpM, gel C) are designated by letter. Open arrows indicate iron-repressible expression only at 26°C, and asterisks identify proteins not produced by Pgm<sup>-</sup> K115-A cells. For gels A and B, iron-replete (lanes 1 and 5) or iron-deficient (lanes 2 to 4 and 6 to 8) cells were grown at 37°C (lanes 1 to 4) or 26°C (lanes 5 to 8). K115+ (Pgm<sup>+</sup> Pst<sup>s</sup>), lanes 1, 2, 5, and 6; K115-B (Hms<sup>+</sup> Pst<sup>t</sup>), lanes 3 and 7; K115-A (Pgm<sup>-</sup> Pst<sup>t</sup>), lanes 4 and 8. For gel C, cells were grown at 26°C in iron-replete medium (K115+, lane 1) or iron-deficient medium (K115+, lane 2; K115-B, lane 3; K115-A, lane 4).

other moderate-strength ferric chelators (nitrilotriacetic acid and sodium PP<sub>i</sub>) and, as previously described (35), inhibition by conalbumin was nearly complete at 37°C. We also confirmed a previous report (35) that *Y. pestis* is unable to utilize iron bound to the hydroxamate siderophore desferrioxamine B at 37°C (Fig. 4). Temperature had a dramatic effect on the ability of *Y. pestis* cells to acquire iron from ferric chelators. For example, growth at 26°C of cells of K115-A and K115-B with conalbumin approached that of K115+ cells. All three strains showed unrestricted growth in the presence of the other ferric chelators at 26°C. The difference was most pronounced for desferrioxamine B, going from no detectable growth at 37°C to complete growth across the gradient at 26°C (Fig. 4). The ferrous chelators (2,2'-dipyridyl and, especially, bathophenanthroline disulfonic acid) strongly inhibited growth at both temperatures. Inhibition by 2,2'-dipyridyl was more severe at both 26 and 37°C for the *Y. pestis* K115-A and K115-B mutants than for K115+ cells (Fig. 4).

**Expression and subcellular localization of iron-repressible proteins.** Both SDS-PAGE (Fig. 1) and 2D gel electrophoresis

(Fig. 5) of subcellular fractions were used to analyze differences in expression of iron-repressible proteins. Fourteen iron-repressible proteins in the OM (IrpS), including HMWP1 and HMWP2, were detected. We were unable to confirm the presence of IrpE (65.1 kDa; isoelectric point, 5.98 [reference 41]), which may be a rarely expressed variant of *psn*. As already noted, *Y. pestis* K115-B did not produce the receptor IrpB to IrpD proteins. Eight more iron-repressible OM proteins (IrpF to IrpM), not encoded within the *pgm* locus, were evident. IrpG to IrpI (36-, 34-, and 28.5-kDa polypeptides, respectively) were better visualized on 2D gels (Fig. 5 and data not shown), while IrpF and IrpJ to IrpL were resolved in lane gels but not in 2D gels. The IrpM group included two or three polypeptides visible in 2D gels, while IrpF and IrpJ to IrpL were evident in lane gels (Fig. 1A). While most Irp proteins were produced at both temperatures, IrpH and IrpI were more highly expressed at 26°C than at 37°C. Conversely, iron-starved expression of IrpJ and IrpK appeared higher at 37°C than at 26°C. IrpK was produced abundantly in all iron-starved cells at 37°C but only in the K115-A mutant at 26°C. IrpF expression in strains

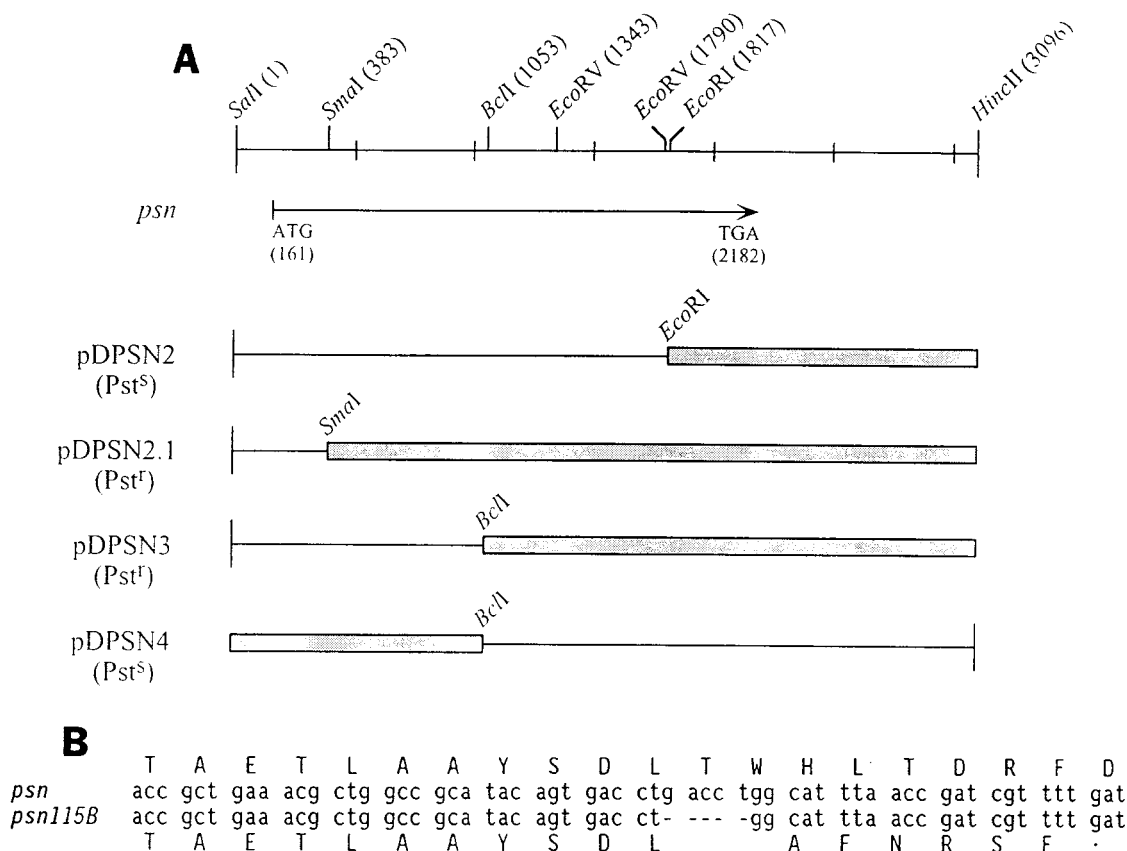


FIG. 2. Comparison of *psn* and *psn115B*. (A) Restriction enzyme map of sequenced *psn* region. Relevant restriction enzyme sites are shown with exact positions (in base pairs) derived from the *psn* sequence (10). Initiating and terminating codons of *psn* are shown. For plasmids containing hybrid *psn*<sup>+</sup>-*psn115B* genes, thick lines denote *psn115B* sequences. The Pst<sup>s</sup> or Pst<sup>t</sup> phenotype of each plasmid is noted. (B) Comparison of *psn* and *psn115B* DNA and amino acid sequences. Only sequences surrounding the mutation in *psn115B* are shown (nucleotides 1286 to 1345 and amino acids 376 to 395 of *psn*).

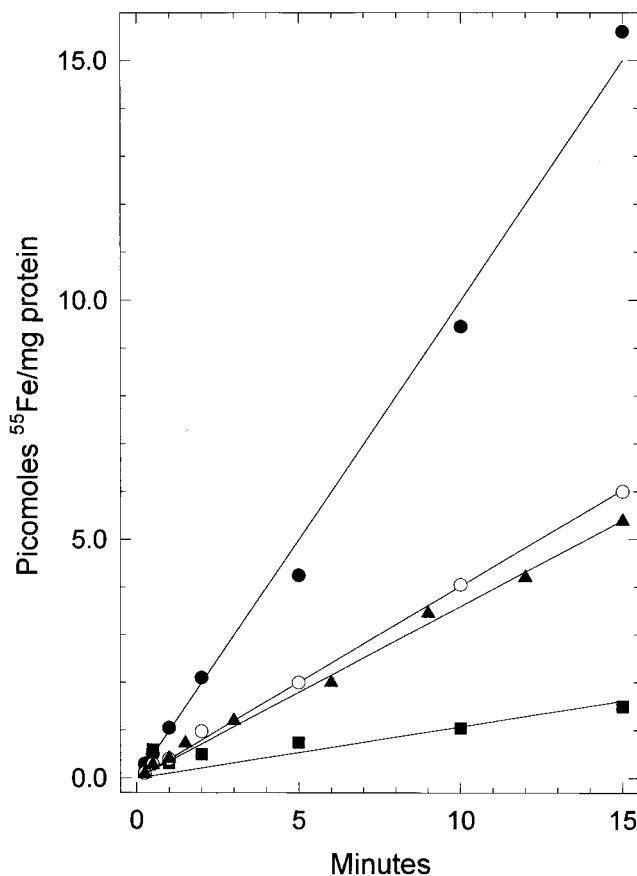


FIG. 3. Acquisition of  $^{55}\text{Fe}^{3+}$  from uptake buffer at  $37^\circ\text{C}$  by cells of *Y. pestis* cultivated for two transfers at  $37^\circ\text{C}$  in modified Higuchi medium. K115+ ( $\text{Pgm}^+$ ) cells were grown in iron-replete medium (■) or iron-deficient medium (●). K115-A ( $\text{Pgm}^- \text{Pst}^+$ ) cells (○) and K115-B ( $\text{Hms}^+ \text{Pst}^+$ ) cells (▲) were grown in iron-deficient medium.

K115-A and K115-B was much weaker at  $26^\circ\text{C}$  than in the K115+ parent and apparently absent at  $37^\circ\text{C}$  (Fig. 1A and Table 2).  $\text{Pgm}$ -related perturbation of iron-regulated proteins has been observed before (42).

Twelve iron-repressible polypeptides (Pirps), as well as HMWP1 and HMWP2, were found in periplasmic samples (Fig. 1B and Table 2). Several of these were among the most strongly expressed proteins in this compartment. PirpG and PirpJ only exhibited high-level expression under iron-deficient conditions at  $26^\circ\text{C}$ . A new  $\text{Pgm}^+$ -specific, iron-repressible protein termed PirpL was identified at 19 kDa. It was clearly visible at  $26^\circ\text{C}$  and usually detectable at  $37^\circ\text{C}$  directly below a more abundant protein with a slightly higher molecular mass. Although PirpL was absent in K115-A cells, it was produced normally in K115-B cells. The HMWP1 and HMWP2 proteins were not produced by K115-A cells (Fig. 1B).

No temperature-dependent differences in any iron-repressible IM polypeptides (Mirps) were observed, and only results from cells grown at  $26^\circ\text{C}$  are illustrated in Fig. 1C. Ten iron-repressible proteins, including HMWP1 and HMWP2, were detected in IM fractions (Fig. 1C and Table 2), and none were  $\text{Pgm}^+$  specific except HMWP1 and HMWP2. High levels of HMWP1 and HMWP2 were also detected in cytoplasmic samples from cells grown under iron-deficient conditions. The remaining polypeptides in this compartment exhibited no iron regulation or strain-dependent expression detectable in lane

gels (data not shown). In contrast to an earlier observation assigning HMWP1 and HMWP2 to the OM, we observed both polypeptides in all subcellular fractions of *Y. pestis* grown at  $26$  or  $37^\circ\text{C}$ . Since most other proteins could be clearly assigned to a specific compartment and the polypeptide profiles of the OM, IM, and periplasm (Fig. 1) were distinct, this result is unlikely to reflect poor separation of fractions during preparation of samples. A summary of the iron-repressible polypeptides detected in this study is presented in Table 2.

## DISCUSSION

Since its initial description (21, 22), the *Y. pestis*  $\text{Pgm}^+$  phenotype has been associated with virulence in mammals, sensitivity to pesticin, iron acquisition, and adsorption of exogenous hemin at  $26$  to  $30^\circ\text{C}$ . Studies have clearly separated the  $\text{Pgm}^+$ -linked iron acquisition system from hemin storage (10, 11, 23, 37, 41) and shown that the pesticin receptor probably functions in iron transport (10, 38). Sikkema and Brubaker (41) first demonstrated a role for the pesticin receptor during growth of *Y. pestis* K115-B in an iron-deficient environment at  $37^\circ\text{C}$ . Our analysis of *Y. pestis* K115-B indicates that it is  $\text{Pst}^+$  because of a 5-bp deletion in *psn115B* that results in an apparently non-functional truncated protein. It is intriguing that this deletion removes one of a pair of tandem direct repeats (Fig. 4B). The *psn* locus appears to be a monocistronic operon, the cloned wild-type *psn* gene complements *in trans*, and the growth defects of K115-B and KIM6-2045.1 (containing an engineered in-frame  $\Delta\text{psn}$  mutation) are similar (10; this study). Accordingly, all phenotypic characteristics of strain K115-B are likely due to this alteration in the *psn115B* gene product.

By using iron transport studies and a number of growth-inhibitory iron chelators, we have clearly demonstrated a correlation between  $\text{Pst}^s$  and iron acquisition. Compared with

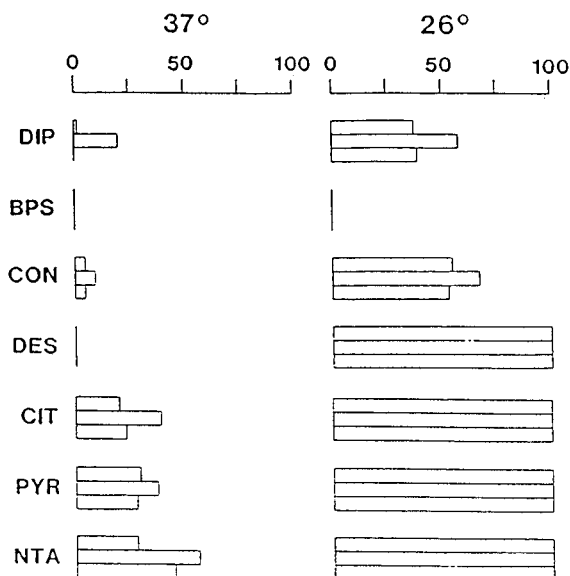
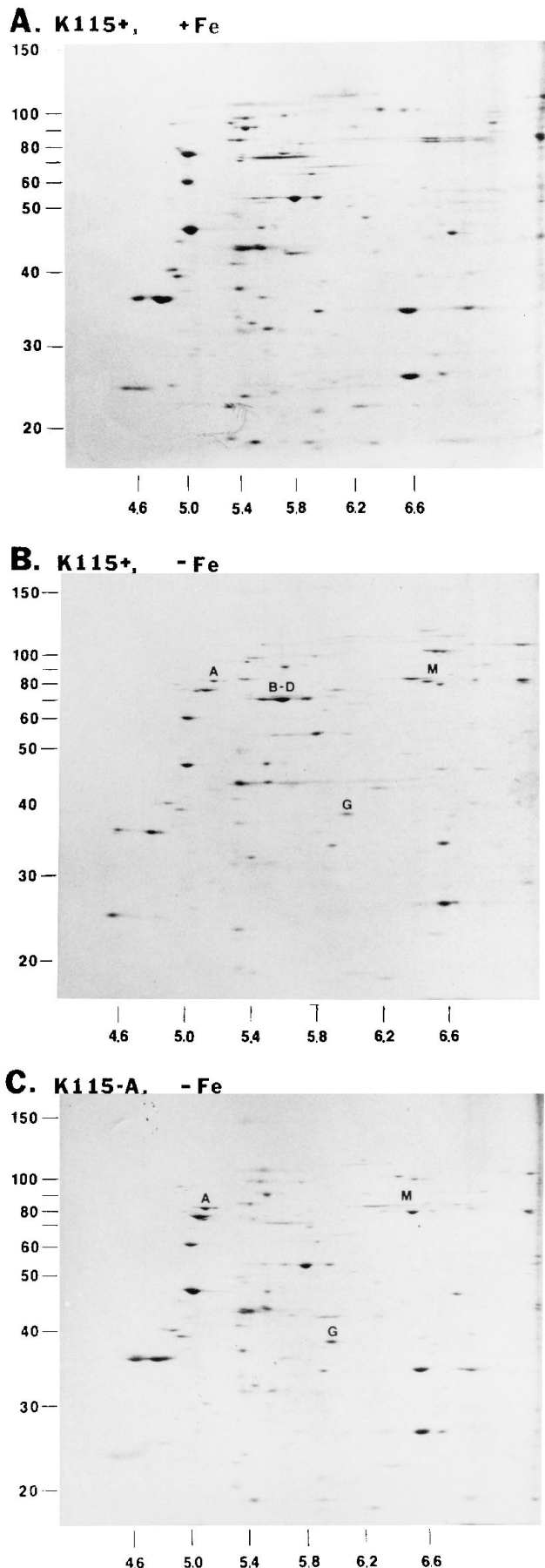


FIG. 4. Growth of *Y. pestis* on iron chelator gradient plates. Rectangles show the distance each streak of cells grew across the iron chelator gradient, from 0 (no growth) to 100 (complete growth across the plate). Iron chelator concentrations are 0 to  $200 \mu\text{M}$  2,2'-dipyridyl (DIP), 0 to  $100 \mu\text{M}$  bathophenanthroline disulfonic acid (BPS), 0 to  $20 \mu\text{M}$  conalbumin (CON), 0 to  $200 \mu\text{M}$  desferrioxamine B (DES), 0 to 1 mM sodium citrate (CIT), 0 to 1 mM sodium  $\text{PP}_i$  (PYR), and 0 to 1 mM sodium nitrilotriacetate (NTA). Results for *Y. pestis* K115-A ( $\text{Pgm}^-$ ) (top rectangle for each chelator), K115+ ( $\text{Pgm}^+$ ) (middle rectangle), and K115-B ( $\text{Hms}^+ \text{Pst}^+$ ) (bottom rectangle) are shown.



$Pgm^+$  cells,  $Pgm^-$  cells, as well as the  $Hms^+$   $Pst^r$  mutants, were more readily inhibited by both ferric and ferrous chelators; for unknown reasons, the latter were more effective inhibitors. The defect in iron-deficient growth associated with  $Pst^r$  could result from impaired iron transport or a metabolic alteration causing a greater requirement for iron. We have demonstrated a  $37^\circ C$ -dependent loss of iron uptake in the  $Pgm^-$  and  $Hms^+$   $Pst^r$  *Y. pestis* mutants and inhibition by citrate of  $Pgm^+$ -linked  $37^\circ C$  acquisition of iron (35; this study). These results and those of other studies suggest that  $Pst^r$  strains do not require more iron for growth but rather are defective in its assimilation.

Previous work has linked IrpB to IrpE and HMWP1 and HMWP2 to the *pgm* locus (10, 11, 41, 42). As noted above, IrpC is the main product of *psn* while IrpB and IrpD appear to be variant forms (10). Since IrpE was not expressed by  $Hms^+$   $Pst^r$  mutant strain K115-B (41), our inability to identify IrpE in this study suggests that it is a rarely expressed variant product of *psn*. Since polypeptides IrpB to IrpE are all encoded by the *psn* gene products and dispense with the earlier, temporary IrpB-to-IrpE nomenclature. *Psn* appears to act as the receptor for an unusual siderophore, while HMWP1 and HMWP2 are likely involved in the biosynthesis of this siderophore (10, 17). We have identified a new  $Pgm^+$ -linked, iron-repressible periplasmic protein (19-kDa PirpL) which is a likely component of this iron acquisition system. Expression of an additional iron-repressible OM polypeptide (113-kDa IrpF) is severely affected by the  $\Delta pgm$  and *psn115B* mutations. No  $Pgm^+$ -linked differences in expression of iron-repressible IM proteins were observed, suggesting that IM components of this iron transport system are masked by proteins with similar molecular weights or are encoded outside of the *pgm* locus. Further work is required to identify all of the biosynthetic and transport components of this iron acquisition system.

It seems plausible that two distinct, *Psn*-independent iron acquisition systems operate—one at  $37^\circ C$  and a second only at  $26^\circ C$ . Evidence favoring the existence of the former was the discovery of increased radioactive ferric iron accumulation in  $Pgm^-$  cells of *Y. pestis* grown at  $37^\circ C$  in iron-deficient media compared with those grown in iron-sufficient media (35; this study). There is substantial evidence of a separate iron transport system functioning at  $26^\circ C$  but not at  $37^\circ C$ . For instance, desferrioxamine B completely inhibited the growth of  $Pgm^+$  and  $Pgm^-$  *Y. pestis* at  $37^\circ C$  but had no significant effect at  $26^\circ C$ . Other iron chelators likewise had less of an effect at  $26^\circ C$  than at  $37^\circ C$  (Fig. 4). In addition, three OM proteins, IrpH, IrpI, and IrpJ, as well as two periplasmic proteins, PirpG and PirpJ, were more highly or exclusively expressed under iron-deficient conditions at  $26^\circ C$ . When uptake of radiolabelled iron was measured,  $Pgm^+$  and  $Pgm^-$  cells grown at  $26^\circ C$  accumulated more iron than did cells grown at  $37^\circ C$  and citrate inhibited this uptake to a much greater extent in cells grown at  $37^\circ C$  (data not shown). It is possible that this system is ineffective because the proteins do not function at  $37^\circ C$ . However, the initial kinetics of iron uptake were more dependent upon the growth temperature of cultures than the uptake assay temperature (data not shown). Consequently, we favor temperature-regulated expression of the genes for this putative iron trans-

FIG. 5. 2D gel comparison of OM polypeptides from *Y. pestis* grown and labelled at  $26^\circ C$  in modified Higuchi medium. OMs from K115+ ( $Pgm^+$ ) iron-replete (A) or iron-deficient (B) cells or from K115-A ( $Pgm^-$ ) iron-deficient cells (C) were separated by 2D gel electrophoresis and visualized by autoradiography. Horizontal isoelectric focusing dimensions are pHs, while vertical SDS-PAGE dimensions are kilodaltons. Letters refer to OM iron-repressible proteins (Irp)s described in Table 2.

TABLE 2. Iron-repressible polypeptides expressed by *Y. pestis* KIM strains

Polypeptide designation <sup>a</sup>	Expression in Pgm <sup>-</sup> strain	Size (kDa)	Subcellular location <sup>b</sup>	Expression temp (°C)
IrpA	Present	80.1	OM	26, 37
IrpB	Absent	68.8	OM	26, 37
IrpC	Absent	67.4	OM	26, 37
IrpD	Absent	69.1	OM	26, 37
IrpF	Absent or down-regulated	113.0	OM	26, 37
IrpG	Present	36.0	OM	26, 37
IrpH	Present	34.0	OM	26
IrpI	Present	28.5	OM	26
IrpJ	Present	22.5	OM	37
IrpK	Present	19.5	OM	37
IrpL	Present	18.8	OM	26, 37
IrpM	Present	80–85	OM	26, 37
HMWP1	Absent	240	OM, PP, IM, C	26, 37
HMWP2	Absent	190	OM, PP, IM, C	26, 37
PirpA	Present	75.0	PP	26, 37
PirpB	Present	39.5	PP	26, 37
PirpC	Present	38.5	PP	26, 37
PirpD	Present	37.7	PP	26, 37
PirpE	Present	37.0	PP	26, 37
PirpF	Present	36.5	PP	26, 37
PirpG	Present	33.7	PP	26
PirpH	Present	31.5	PP	26, 37
PirpI	Present	31.0	PP	26, 37
PirpJ	Present	30.0	PP	26
PirpK	Present	25.0	PP	26, 37
PirpL	Absent	19.0	PP	26, 37
MirpA	Present	127.0	IM	26, 37
MirpB	Present	115.0	IM	26, 37
MirpC	Present	94.0	IM	26, 37
MirpD	Present	55.5	IM	26, 37
MirpE	Present	36.0	IM	26, 37
MirpF	Present	35.0	IM	26, 37
MirpG	Present	33.0	IM	26, 37
MirpH	Present	29.8	IM	26, 37

<sup>a</sup> Irp, Pirp, and Mirp designations are temporary nomenclature for OM, periplasmic, and IM iron-repressible polypeptides that will be replaced as the functions of these polypeptides are identified. IrpB to IrpE are all encoded by *psn* and will subsequently be termed Psn.

<sup>b</sup> PP, periplasm; C, cytoplasm.

port system as the explanation for temperature-dependent function. The mechanism of iron uptake by either of these two putative acquisition systems is completely undetermined.

We initiated an evaluation of iron-repressible proteins in *Y. pestis* to identify possible iron acquisition proteins and other iron-regulated virulence factors. We identified and localized 32 iron-repressible (IrpB to IrpE [Psn] and IrpM groups each counting as one) proteins. Fractionation of cells allowed us to detect iron-repressible proteins that may have been masked in other determinations (42). For this and other reasons, it is difficult to unambiguously correlate iron-repressible polypeptides identified in this study with those detected by Staggs et al. (42). Indeed, our analysis was not comprehensive; neither the cytoplasmic iron-regulated Fur protein nor a known 56-kDa protein was detected (10, 42). These differences may be due to different culture conditions or different analytical protocols. However, we did identify an additional Pgm<sup>+</sup>-linked iron-repressible polypeptide, PirpL, in the periplasm. Pgm<sup>+</sup>-linked iron-repressible proteins now include Psn (formerly termed

IrpB to IrpE), PirpL, HMWP1, HMWP2, and a 56-kDa protein which may be involved in the Psn-dependent acquisition of iron. Our cellular fractionation method indicates that HMWP1 and HMWP2 are present in all cellular compartments and suggests that they span the cell envelope and extend into the cytoplasm. Destruction of the IM structure by Triton X-100 may account for the previous localization of these two proteins to the OM (4, 16). Of the remaining 9 OM, 11 periplasmic, and 8 IM iron-repressible polypeptides encoded outside the *pgm* locus, several have intriguing characteristics. The group more highly expressed at 26°C are candidates for the putative 26°C transport system. IrpK and IrpL were more highly expressed at 37°C. Regulated expression of IrpF and IrpK was perturbed by the  $\Delta$ *pgm* or *psn115B* mutation. Undoubtedly, a number of these proteins are involved in iron acquisition while others may represent virulence proteins not concerned with iron accumulation but using iron starvation as an environmental sensor. The *Y. pestis* strains examined here lack both the low-calcium response and pesticin-plasminogen activator plasmids which may encode additional iron-repressible functions (40, 41). None of the new iron-repressible polypeptides described here correspond to known virulence proteins in yersiniae; the functions of nearly all of these proteins remain to be resolved.

#### ACKNOWLEDGMENTS

This work was supported by Public Health Service grants AI33481 (J.D.F. and R.D.P.) and AI19353 (R.R.B.) from the National Institutes of Health.

We thank Matthew L. Wilson for assistance in localizing the mutation in the defective *psn115B* gene of *Y. pestis* K115-B, as well as Heather Jones and Janet M. Fowler for assistance with several experiments.

#### REFERENCES

- Ausubel, F. M., R. Brent, R. E. Kingston, D. D. Moore, J. G. Seidman, J. A. Smith, and K. Struhl (ed.). 1987. Current protocols in molecular biology. John Wiley & Sons, Inc., New York.
- Birnboim, H. C., and J. Doly. 1979. A rapid alkaline extraction procedure for screening recombinant plasmid DNA. *Nucleic Acids Res.* 7:1513–1523.
- Brubaker, R. R. 1969. Mutation rate to nonpigmentation in *Pasteurella pestis*. *J. Bacteriol.* 98:1404–1406.
- Carniel, E., J.-C. Antoine, A. Guiyoule, N. Guiso, and H. H. Mollaret. 1989. Purification, location, and immunological characterization of the iron-regulated high-molecular-weight proteins of the highly pathogenic yersiniae. *Infect. Immun.* 57:540–545.
- Carniel, E., D. Mazigh, and H. H. Mollaret. 1987. Expression of iron-regulated proteins in *Yersinia* species and their relation to virulence. *Infect. Immun.* 55:277–280.
- Carniel, E., O. Mercereau-Puijalon, and S. Bonnefoy. 1989. The gene coding for the 190,000-Dalton iron-regulated protein of *Yersinia* species is present only in the highly pathogenic strains. *Infect. Immun.* 57:1211–1217.
- Cornelissen, C. N., and P. F. Sparling. 1994. Iron piracy: acquisition of transferrin-bound iron by bacterial pathogens. *Mol. Microbiol.* 14:843–850.
- Cox, C. D. 1980. Iron uptake with ferripyochelin and ferric citrate by *Pseudomonas aeruginosa*. *J. Bacteriol.* 142:581–587.
- Earhart, C. F. 1987. Ferrienterobactin transport in *Escherichia coli*, p. 67–84. *In* G. Winkelmann, D. van der Helm, and J. B. Neilands (ed.), Iron transport in microbes, plants and animals. VCH Publishers, New York.
- Fetherston, J. D., J. W. Lillard, Jr., and R. D. Perry. 1995. Analysis of the pesticin receptor from *Yersinia pestis*: role in iron-deficient growth and possible regulation by its siderophore. *J. Bacteriol.* 177:1824–1833.
- Fetherston, J. D., and R. D. Perry. 1994. The pigmentation locus of *Yersinia pestis* KIM6+ is flanked by an insertion sequence and includes the structural genes for pesticin sensitivity and HMWP2. *Mol. Microbiol.* 13:697–708.
- Fetherston, J. D., P. Schuetze, and R. D. Perry. 1992. Loss of the pigmentation phenotype in *Yersinia pestis* is due to the spontaneous deletion of 102 kb of chromosomal DNA which is flanked by a repetitive element. *Mol. Microbiol.* 6:2693–2704.
- Griffiths, E. 1987. The iron-uptake systems of pathogenic bacteria, p. 69–137. *In* J. J. Bullen and E. Griffiths (ed.), Iron and infection. Molecular, physiological and clinical aspects. John Wiley & Sons, Inc., New York.
- Grunstein, M., and D. S. Hogness. 1975. Colony hybridization: a method for the isolation of cloned DNAs that contain a specific gene. *Proc. Natl. Acad. Sci. USA* 72:3961–3965.



15. Guerinot, M. L. 1994. Microbial iron transport. *Annu. Rev. Microbiol.* **48**:743–772.
16. Guilvout, I., E. Carniel, and A. P. Pugsley. 1995. *Yersinia* spp. HMWP2, a cytosolic protein with a cryptic internal signal sequence which can promote alkaline phosphatase export. *J. Bacteriol.* **177**:1780–1787.
17. Guilvout, I., O. Mercereau-Puijalon, S. Bonnefoy, A. P. Pugsley, and E. Carniel. 1993. High-molecular-weight protein 2 of *Yersinia enterocolitica* is homologous to AngR of *Vibrio anguillarum* and belongs to a family of proteins involved in nonribosomal peptide synthesis. *J. Bacteriol.* **175**:5488–5504.
18. Hornung, J. M., H. A. Jones, and R. D. Perry. 1996. The *hmu* locus of *Yersinia pestis* is essential for utilization of free haemin and haem-protein complexes as iron sources. *Mol. Microbiol.* **20**:725–739.
19. Humphreys, G. O., G. A. Willshaw, and E. S. Anderson. 1975. A simple method for the preparation of large quantities of pure plasmid DNA. *Biochim. Biophys. Acta* **383**:457–463.
20. Iteman, I., A. Guiyoule, A. M. P. de Almeida, I. Guilvout, G. Baranton, and E. Carniel. 1993. Relationship between loss of pigmentation and deletion of the chromosomal iron-regulated *irp2* gene in *Yersinia pestis*: evidence for separate but related events. *Infect. Immun.* **61**:2717–2722.
21. Jackson, S., and T. W. Burrows. 1956. The pigmentation of *Pasteurella pestis* on a defined medium containing haemin. *Br. J. Exp. Pathol.* **37**:570–576.
22. Jackson, S., and T. W. Burrows. 1956. The virulence enhancing effect of iron on non-pigmented mutants of virulent strains of *Pasteurella pestis*. *Br. J. Exp. Pathol.* **37**:577–583.
23. Kuttyrev, V. V., A. A. Filippov, O. S. Oparina, and O. A. Protsenko. 1992. Analysis of *Yersinia pestis* chromosomal determinants Pgm<sup>+</sup> and Pst<sup>s</sup> associated with virulence. *Microb. Pathog.* **12**:177–186.
24. Lee, B. C. 1995. Quelling the red menace: haem capture by bacteria. *Mol. Microbiol.* **18**:383–390.
25. Lowry, O. H., N. J. Rosebrough, A. L. Farr, and R. J. Randall. 1951. Protein measurement with the Folin phenol reagent. *J. Biol. Chem.* **193**:265–275.
26. Lucier, T. S., and R. R. Brubaker. 1992. Determination of genome size, macrorestriction pattern polymorphism, and nonpigmentation-specific deletion in *Yersinia pestis* by pulsed-field gel electrophoresis. *J. Bacteriol.* **174**:2078–2086.
27. Mietzner, T. A., and S. A. Morse. 1994. The role of iron-binding proteins in the survival of pathogenic bacteria. *Annu. Rev. Nutr.* **14**:471–493.
28. Morrissey, J. H. 1981. Silver stain for proteins in polyacrylamide gels: a modified procedure with enhanced uniform sensitivity. *Anal. Biochem.* **117**:307–310.
29. Neilands, J. B., K. Konopka, B. Schwyn, M. Coy, R. T. Francis, B. H. Paw, and A. Bagg. 1982. Microbial envelope proteins related to iron. *Annu. Rev. Microbiol.* **36**:285–309.
30. O'Farrell, P. H. 1975. High resolution two-dimensional electrophoresis of proteins. *J. Biol. Chem.* **250**:4007–4021.
31. Payne, S. M. 1988. Iron and virulence in the family Enterobacteriaceae. *Crit. Rev. Microbiol.* **16**:81–111.
32. Pendrak, M. L., and R. D. Perry. 1990. Characterization of a hemin-storage locus of *Yersinia pestis*. *Biol. Metals* **4**:41–47.
33. Pendrak, M. L., and R. D. Perry. 1993. Proteins essential for expression of the Hms<sup>+</sup> phenotype of *Yersinia pestis*. *Mol. Microbiol.* **8**:857–864.
34. Perry, R. D. 1993. Acquisition and storage of inorganic iron and hemin by the yersiniae. *Trends Microbiol.* **1**:142–147.
35. Perry, R. D., and R. R. Brubaker. 1979. Accumulation of iron by yersiniae. *J. Bacteriol.* **137**:1290–1298.
36. Perry, R. D., T. S. Lucier, D. J. Sikkema, and R. R. Brubaker. 1993. Storage reservoirs of hemin and inorganic iron in *Yersinia pestis*. *Infect. Immun.* **61**:32–39.
37. Perry, R. D., M. L. Pendrak, and P. Schuetze. 1990. Identification and cloning of a hemin storage locus involved in the pigmentation phenotype of *Yersinia pestis*. *J. Bacteriol.* **172**:5929–5937.
38. Rakin, A., E. Saken, D. Harmsen, and J. Heesemann. 1994. The pesticin receptor of *Yersinia enterocolitica*: a novel virulence factor with dual function. *Mol. Microbiol.* **13**:253–263.
39. Sambrook, J., E. F. Fritsch, and T. Maniatis. 1989. *Molecular cloning: a laboratory manual*, 2nd ed. Cold Spring Harbor Laboratory Press, Cold Spring Harbor, N.Y.
40. Sikkema, D. J., and R. R. Brubaker. 1987. Resistance to pesticin, storage of iron, and invasion of HeLa cells by yersiniae. *Infect. Immun.* **55**:572–578.
41. Sikkema, D. J., and R. R. Brubaker. 1989. Outer membrane peptides of *Yersinia pestis* mediating siderophore-independent assimilation of iron. *Biol. Metals* **2**:174–184.
42. Staggs, T. M., J. D. Fetherston, and R. D. Perry. 1994. Pleiotropic effects of a *Yersinia pestis fur* mutation. *J. Bacteriol.* **176**:7614–7624.
43. Staggs, T. M., and R. D. Perry. 1991. Identification and cloning of a *fur* regulatory gene in *Yersinia pestis*. *J. Bacteriol.* **173**:417–425.
44. Staggs, T. M., and R. D. Perry. 1992. Fur regulation in *Yersinia* species. *Mol. Microbiol.* **6**:2507–2516.
45. Straley, S. C., and R. R. Brubaker. 1981. Cytoplasmic and membrane proteins of yersiniae cultivated under conditions simulating mammalian intracellular environment. *Proc. Natl. Acad. Sci. USA* **78**:1224–1228.
46. Straley, S. C., and R. R. Brubaker. 1982. Localization in *Yersinia pestis* of peptides associated with virulence. *Infect. Immun.* **36**:129–135.
47. Surgalla, M. J., and E. D. Beesley. 1969. Congo red-agar plating medium for detecting pigmentation in *Pasteurella pestis*. *Appl. Microbiol.* **18**:834–837.
48. Une, T., and R. R. Brubaker. 1984. In vivo comparison of avirulent Vwa<sup>-</sup> and Pgm<sup>-</sup> or Pst<sup>r</sup> phenotypes of yersiniae. *Infect. Immun.* **43**:895–900.
49. Way, J. C., M. A. Davis, D. Morisato, D. E. Roberts, and N. Kleckner. 1984. New Tn10 derivatives for transposon mutagenesis and for construction of *lacZ* operon fusions by transposition. *Gene* **32**:369–379.
50. Zahorchak, R. J., and R. R. Brubaker. 1982. Effect of exogenous nucleotides on Ca<sup>2+</sup> dependence and V antigen synthesis in *Yersinia pestis*. *Infect. Immun.* **38**:953–959.

Editor: B. I. Eisenstein